A small molecule in metal cluster cages: $H_2@Mg_n$ (n = 8 to 10)

Phillip McNelles and Fedor Y. Naumkin*

Received 4th November 2008, Accepted 24th February 2009
First published as an Advance Article on the web 4th March 2009
DOI: 10.1039/b819479c

Core-shell isomers of small magnesium clusters "doped" with a hydrogen molecule are theoretically studied and predicted to be weakly stable or metastable for different sizes of the system, allowing a low-temperature release of hydrogen. Evolution of H_2 inside Mg_n is followed from the molecular species to two H atoms. Among properties analyzed are equilibrium geometries, dissociation energies, charge distributions, vertical energies of electronic excitation, ionization and electron attachment, and vibrational frequencies.

Introduction

Atomic clusters of some metals are theoretically and experimentally found to have isomers in the form of cage structures with empty spaces inside, such as Au_{16}, Au_{18},[1] *etc*. Smaller examples include commonly found bi-pyramids with trigonal, square, pentagonal bases, such as, *e.g.*, Mg_n clusters.[2,3] Metal clusters of open-shell atoms are of interest as, in particular, catalytic agents, and gold is an object of increased attention recently,[4] with the potential of catalysis inside cages to be evaluated yet. Clusters of chemically more inert, closed-subshell atoms, such as magnesium, *etc*, could be viewed as potential candidates for molecular storage applications. In the present work, small magnesium cluster cages are investigated from the viewpoint of trapping a single hydrogen molecule (and, interestingly, found to exhibit some endohedral catalytic activity as well).

In particular, magnesium hydride MgH_2 is a material considered in terms of massive hydrogen storage, one difficulty being the high temperatures needed to extract hydrogen from the solid's bulk.[5] Hydrogen desorption is found to occur at lower temperatures in the small grains (clusters) of this material.[6] Furthermore, recent studies[7] indicate a catalytic reduction of the dehydrogenation energies in MgH_2 nanoclusters doped with transition metals such as Fe. Here we preliminarily study systems with non-covalent interactions between H_2 and the surrounding Mg_n shell, originating from the weakly bound $Mg\cdots H_2$ isomer and thus potentially facilitating an easier release of hydrogen.

Computational procedure

In order to reliably deal with the weakly-bound systems of appreciable size, calculations have been performed at the MP2 level with aug-cc-pVDZ (hereafter avdz) basis sets[8] for all atoms, by means of the NWChem software.[9] At this level, the equilibrium distances R_e of H_2 and Mg_2 are, respectively, 0.75 and 4.39 Å, to be compared with experimental 0.74 and 3.89 Å,[10] and the corresponding dissociation energies D_e are 4.3 and 0.036 eV, close to 4.52 and 0.049 eV from experiments. The calculated Mg ionization energy is 7.23 eV, within 6% of the experimental value of 7.65 eV.

The significant deviation of predicted and measured equilibrium parameters for Mg_2 is due to a very shallow potential well, and would increase even further with the basis set superposition error correction (BSSEC). For a larger aug-cc-pVTZ (avtz) basis set,[8] bonding in Mg_2 is significantly overestimated before BSSEC, while a single-point BSSEC at this too-short R_e (without re-optimization) gives a lower bound of D_e slightly under the no-BSSEC avdz-value. Fortunately, the situation quickly improves with increasing size of Mg_n clusters (Table 1). Not only the avtz (with BSSEC) lower-bound D_e is accurately reproduced by the avdz (without BSSEC) value, but also the R_e values converge for both basis sets (to within 1% for Mg_4). This justifies using the avdz basis set and limiting the BSSEC for the systems of interest (with $n > 4$) to a single-point (vertical) avtz calculation at avdz-R_e, as confirmed by so produced D_e estimates for Mg_n (n = 2–4) being almost identical to those at avtz-R_e. In particular, present results for Mg_3 and Mg_4 favourably compare with higher-level CCSD(T) data.[11]

Full unconstrained optimizations of geometry have been carried out for all systems. Subsequent vibrational-frequency calculations have been employed also to confirm local energy-minima. The obtained structures have been visualized using the ViewMol3D software.[12] Charge distributions are characterized in terms of natural charges on atoms.

Results and discussion

Out of various Mg_n clusters,[2,3] those with suitable cage structures (potentially able to accommodate a hydrogen diatom inside) in their ground states have been used, such as Mg_5 trigonal and Mg_7 pentagonal bi-pyramids and Mg_9 triply capped (equilateral) trigonal prism. Upon optimization of these cluster structures, the H_2 molecule has been inserted inside centrally, with a few different orientations, typically along the symmetry axis of the cage and in two perpendicular directions. The Mg_5 and Mg_7 cages are found to be too tight to accommodate the molecule, and to break, releasing it, upon optimization.

The Mg_9 cage is found to successfully trap H_2 oriented perpendicular to the cage axis, while the structure with H_2 along the axis corresponds to a transition state. Upon relaxation, the cage structure somewhat alters and becomes a "cup" composed of two staggered squares, capped on one side

Faculty of Science, UOIT, Oshawa, Canada ON L1H 7K4. E-mail: fedor.naumkin@uoit.ca; Fax: +1 905 7213304

 This journal is © the Owner Societies 2009

Table 1 Equilibrium parameters (in eV and Å) of small Mg_n

System	D_e (avdz)	R_e (avdz)	D_e (avtz)[a]	R_e (avtz)	D(avtz)[a] @ R_e(avdz)
Mg_2	0.036	4.39	0.117/0.031	3.74	0.096/0.039
Mg_3[b]	0.22	3.38	0.58/0.23	3.22	0.56/0.25
Mg_4[c]	1.20	3.03	1.91/1.20	2.99	1.91/1.20

[a] Without/with BSSEC (at no-BSSEC geometry). [b] Equilateral-triangular. [c] Tetrahedral. avdz/avtz stand for aug-cc-pVDZ/-pVTZ.

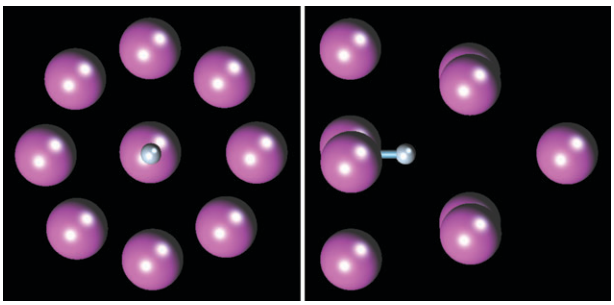

Fig. 1 Optimized structure of $H_2@Mg_9$: front (left) and side (right) views.

(Fig. 1), with the molecule positioned along its axis closer to the non-capped side. The H–H bond in $H_2@Mg_9$ is significantly stretched relative to the isolated molecule (by $\approx$0.2 Å). The system is bound on average by $\approx$0.6 eV per Mg atom (about same as for original Mg_9), and has a low dissociation energy relative to separated (relaxed) cluster cage and dihydrogen (Table 2). The latter D_e value becomes even negative upon the approximate BSSEC (see Computational procedure), indicating a possibility of the system being slightly metastable. If axially shifted to protrude from the "cup", the molecule is pulled back inside upon relaxation, indicating a potential barrier to such dissociation (*i.e.* release of H_2), hence an extra stability.

Taking away the capping Mg atom in $H_2@Mg_9$ produces symmetric $H_2@Mg_8$ with the dihydrogen in the centre of the staggered-squares cage (Fig. 2). This is consistent with the molecule being repelled from capping Mg at the distance shorter than the equilibrium value of 4.24 Å in the linear Mg–H_2 complex (calculated to be bound by $\approx$0.01 eV). The same geometry is obtained when H_2 is inserted into the isolated Mg_8 cluster (of quite a different initial shape). The cage in $H_2@Mg_8$ is slightly more stretched than in $H_2@Mg_9$, regarding both the Mg_4 square size and the distance between them (Table 2). The molecule is somewhat shorter (by $\approx$0.1 Å) as compared to the $H_2@Mg_9$ case. The Mg_8H_2 system is predicted to be slightly metastable relative to relaxed H_2 and Mg_8 (capped Mg_7[2,3]), with a small negative D_e value. The BSSEC somewhat increases the metastability.

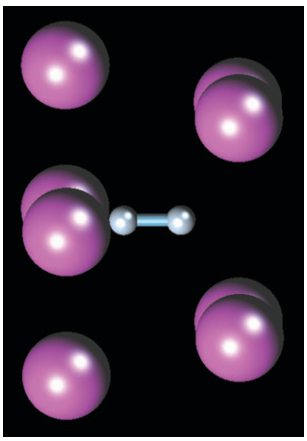

Fig. 2 Optimized structure of $H_2@Mg_8$.

Adding a second capping Mg atom on the opposite side of $H_2@Mg_9$ creates a symmetric $H_2@Mg_{10}$ system with the dihydrogen trapped inside. The molecule, however, dissociates (Fig. 3), apparently due to a further, critical stretch of its bond in the anionic state (as discussed below). The separate H atoms occupy symmetric positions approximately at the centres of the Mg_4 squares which slightly shrink as compared to Mg_9H_2 (Table 2). All Mg–H distances remain well above 1.73 Å (the equilibrium value for the MgH diatom as calculated here in agreement with experiments[10]) as well as above 1.87 Å for MgH^-. The cage shape is considerably different from that of isolated Mg_{10} (which is capped Mg_9), though recovering it when H_2 is removed. The $H_2@Mg_{10}$ is found to be metastable, with energy somewhat above that of (relaxed) Mg_{10} and H_2, this energy difference further increasing with the BSSEC. Binding energies of $H_2@Mg_n$ per Mg atom somewhat increase from n = 8 to 10. Test re-optimizations with the avtz basis set show only minor geometry variations in any atom–atom distance within 0.03 Å—for all $H_2@Mg_n$ (n = 8–10).

Removing one capping atom from $H_2@Mg_{10}$ leads to another isomer of $H_2@Mg_9$, with dissociated dihydrogen (Fig. 4). The H atoms are somewhat more apart than in the $H_2@Mg_{10}$ case and slightly shifted from the Mg_4 square centres towards the "exit" from the "cup". The Mg_9 cage

Table 2 Equilibrium parameters (in eV and Å) of $H_2@Mg_n$ systems

System	D_e[a]	R_e(H–H)	R_e(Mg–H)	R_e(Mg–Mg)
$H_2@Mg_8$	−0.09/−0.27, 3.40/3.30	0.84	2.45	3.25, 3.09[c]
$H_2@Mg_9$	0.11/−0.16, 5.56/5.14	0.93	2.24, 2.61, 3.41[b]	3.15, 3.04[c], 3.03[d]
with dissociated H_2	0.39/−0.05, 5.84/5.25	2.44	2.21, 2.36, 2.54[b]	2.97/3.19[e], 2.94[c], 2.93[d]
$H_2@Mg_{10}$	−0.42/−0.76, 7.56/6.97	2.31	2.18, 2.13[b]	3.08, 2.99[c], 2.99[d]

[a] $H_2@Mg_n \rightarrow H_2 + Mg_n$, $\rightarrow H_2 + n$Mg without/with the vertical BSSEC using avtz basis set at avdz geometry. [b] For the capping atom. [c] Between the Mg_4 squares. [d] Between the capping atom and the Mg_4 square. [e] For non-capped/capped Mg_4 square.

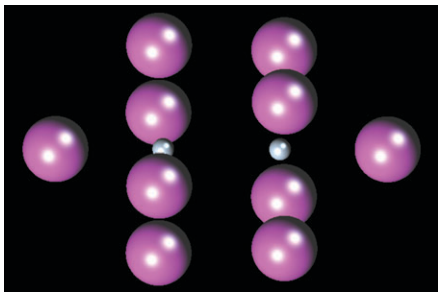

Fig. 3 Optimized structure of $H_2@Mg_{10}$.

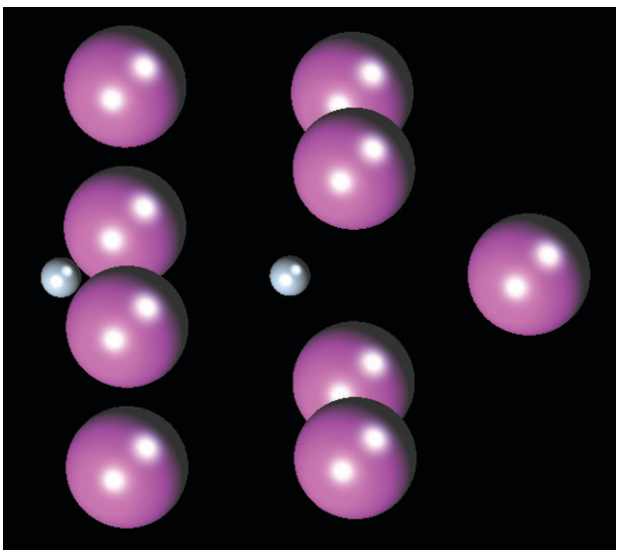

Fig. 4 Optimized structure of the $H_2@Mg_9$ isomer with dissociated H_2.

slightly shrinks along the axis and the Mg_4 squares differ in size, the capped one being somewhat larger (Table 2). The barrier to the H_2 dissociation inside the Mg_9 cage is calculated to be low, at $\approx$0.1 eV. This $H_2@Mg_9$ isomer has a lower energy than that with non-dissociated H_2. The BSSEC makes the system marginally metastable, similar to the case of the first Mg_9H_2 isomer. Locking the dihydrogen inside the Mg_{10} cage thus removes the barrier to its dissociation and produces an extra strain in the system (the cage is too tight). The $Mg–H_2@Mg_{n-1}$ (n = 9,10) binding energy is $\approx$2 eV.

The evolution of the molecule bond length and of the cage size in $H_2@Mg_n$ from n = 8 to 10 is consistent with the natural charge distributions. The dihydrogen is calculated to be increasingly negative (hence less bonded—due to occupation of its antibonding orbital) in this row, up to forming two atomic anions in $H_2@Mg_{10}$ (Table 3). Indeed, for an "initial" geometry of this system with the same H–H distance as in the first $H_2@Mg_9$ isomer, the charges on the H atoms are −0.61e each, *i.e.* larger than in $H_2@Mg_9$, leading to what could be viewed as a Coulomb explosion of the dihydrogen confined in the metal cage. The hydrogens in $H_2@Mg_9$ are more negative in the second isomer, likely due to higher electronegativity of the open-shell H atoms (same for $H_2@Mg_{10}$).

The steady increase of the charge-transfer in $H_2@Mg_n$ with n can be associated with increasing number of metal atoms donating electrons. From n = 8 to 10, the matching (also increasing) positive charge on the cage contracts it more and more strongly around the negative central molecule. The axial Mg atoms (for n = 9, 10) are about twice as positive as those in the Mg_4 squares. In $H_2@Mg_{10}$, no appreciable electron density is found between each H^- and neighbouring Mg atoms. Being asymmetric along its axis, $H_2@Mg_9$ has a small dipole moment of $\approx$0.19 D for the first isomer but essentially none ($\approx$0.03 D) for the isomer with dissociated H_2.

All above $H_2@Mg_n$ systems are closed shell species, with the triplet states higher in energy by one to a few eV (Table 4). The gap increases with n and nearly doubles from n = 8 to 9 while adding further 20% for n = 10. The vertical ionization energies follow the same overall trend, while increasing slightly from n = 8 to 9 and significantly from n = 9 to 10. This can be related to a similar variation of the molecule-cage charge separation (Table 3), as well as to (magic) 20 electrons in the Mg_{10} cluster or, at least, 18 electrons in the Mg_{10}^{2+} cage. The vertical electron affinities are low for all species, being even negative for $H_2@Mg_8$ and $H_2@Mg_9$. All values are somewhat smaller for the second $H_2@Mg_9$ isomer. Investigation of structure relaxation and related charge redistribution following these electronic perturbations is beyond the scope of the present work.

Calculated vibrational frequencies for IR-intense modes are listed in Table 5. The IR intensities increase considerably from $H_2@Mg_8$ to $H_2@Mg_{10}$, generally following the variation of the charge separation between the dihydrogen and the cage. The same is valid for the frequencies as well. For $H_2@Mg_8$ and $H_2@Mg_{10}$, the three most IR-active modes correspond to the dihydrogen oscillating as a whole along the system axis (z) and in two equivalent perpendicular directions (x and y). For $H_2@Mg_9$, the similar axial mode is the most IR-intense one as well, followed by perpendicular modes involving also rocking and swivelling of H_2 (due to asymmetry along the axis). For the $H_2@Mg_9$ isomer with dissociated H_2, the (still most IR-intense) axial mode includes also stretching of H_2.

Each of $H_2@Mg_8$ and $H_2@Mg_9$ exhibits a highest frequency (well isolated from others), respectively, $\approx$2810 and $\approx$1990 cm^{-1}, correlating to (predominantly) H_2 stretch. For $H_2@Mg_{10}$ and second $H_2@Mg_9$ isomer the corresponding frequencies of 891 and 763 cm^{-1} (not isolated) are much lower, reflecting the dissociated state of the molecule.

Table 3 Natural atomic charges (in e) in $H_2@Mg_n$ systems

System	q(H)	q(Mg)
$H_2@Mg_8$	−0.15	−0.10 to +0.18
$H_2@Mg_9$	−0.35[a], −0.40	4 × 0.095[a], 4 × 0.053, 0.17[b]
with dissociated H_2	−0.85[a], −0.98	4 × 0.20[a], 4 × 0.16, 0.38[b]
$H_2@Mg_{10}$	−0.97	8 × 0.16, 2 × 0.31[b]

[a] At the non-capped side. [b] For the capping atom.

Table 4 Vertical energies (in eV) of $H_2@Mg_n$ systems

System	VE*(S = 0 → 1)	VIE	VEA
$H_2@Mg_8$	1.31	5.80	−0.21
$H_2@Mg_9$	2.44	6.08	−0.33
with dissociated H_2	2.05	5.85	−0.09
$H_2@Mg_{10}$	3.00	7.31	0.09

This journal is © the Owner Societies 2009

Table 5 Selected vibrational frequencies (in cm^{-1}), IR intensities ($D^2/Å^2$) of $H_2@Mg_n$

System	ν	I
$H_2@Mg_8$	402, 2 × 409	0.70, 2 × 0.34
$H_2@Mg_9$	436, 541, 543, 717, 721, 1988	2.84, 0.90, 1.04, 0.68, 1.05, 0.61
with dissociated H_2	2 × 522, 553, 763	2 × 4.81, 7.11, 1.06
$H_2@Mg_{10}$	2 × 770, 817	2 × 13.8, 54.5

These values show a dramatic red-shift, increasing in the $H_2@Mg_8$ to $H_2@Mg_{10}$ row, from ≈4460 cm^{-1} for isolated H_2 (experimental 4400 cm^{-1}) due to a strong, charge-transfer assisted interaction of the molecule with the much heavier cage. Due to the asymmetry of $H_2@Mg_9$, the H_2-stretch is significantly IR-active in this system (Table 5).

Conclusions

Aggregates of a hydrogen molecule with small magnesium clusters are predicted (at the MP2 level) to have $H_2@Mg_n$ isomers with the dihydrogen trapped inside the metal cage. The H_2 core significantly re-structures the surrounding Mg_n shell *via* strong interaction between these oppositely charged components. The molecule steadily stretches from $n = 8$ to 10, still preserving its integrity in $H_2@Mg_8$ and $H_2@Mg_9$ while dissociating in $H_2@Mg_{10}$, due to increasing electron donation from the cage. This may serve as an example of a molecule dissociation catalyzed by the metal cluster-cage environment.

The dihydrogen may thus be stored inside the metal cluster in either dissociated or non-dissociated form. It should be noted that the weight-efficiency of such a storage is low (∼1% of hydrogen). Future work will be aimed at increasing the hydrogen content. Further analysis of such storage feasibility should include paths and associated barriers for H_2 entering and exiting the metal cage, which is beyond the scope of the present work. One idea for $H_2@Mg_9$ is the molecule entering through the side of the trigonal prism between two capping atoms and leaving through the non-capped end of the "cup".

The system stability to dissociation into $H_2 + Mg_n$ varies with size (n) from weakly metastable $H_2@Mg_8$ and $H_2@Mg_{10}$ to weakly bound or perhaps slightly metastable (both at ∼0.1 eV scale) $H_2@Mg_9$. The charge-transfer stabilization can thus be compensated by the molecule and cage deformations, potentially allowing a relatively easy release of hydrogen. In fact, the systems may actually survive only at low temperatures.

It should be noted that metastability of $H_2@Mg_n$, obtained with the BSSEC, could be overestimated, since this correction has been evaluated for neutral H_2 and Mg_n (as proper dissociation products) while they are significantly charged in $H_2@Mg_n$. This is supported by the BSSEC effect increasing with the charge value. Anyway, if the systems were indeed metastable, it could facilitate the release of hydrogen.

The results can be somewhat sensitive to the theory level used. In particular, additional DFT(B3LYP) calculations with the same basis set confirm same shapes of $H_2@Mg_n$ (n = 8–10) while predicting all these species to be metastable (by ≈0.5–1 eV even before BSSEC) and showing no barrier-less dissociation of H_2 inside the Mg_{10} cage. The MP2 predictions are believed to be more accurate, since DFT/B3LYP significantly (by ≈50%) underestimates the Mg–Mg binding, as found previously as well.[2]

The closed-shell $H_2@Mg_n$ species, for $n = 10$ particularly, also show stability in terms of electronic (triplet) excitation, ionization and electron-attachment, which could favour their low chemical reactivity and efficient formation in experiments. Their detection can be assisted by high IR intensities of the vibrational modes associated with relative translations of the oppositely charged dihydrogen and cage.

Acknowledgements

FN acknowledges financial support of the NSERC of Canada (Discovery grant). Authors appreciate technical support of the staff of high-performance computing facilities of the UOIT Faculty of Science and of the SHARCnet distributed academic network of Ontario.

References

1 S. Bulusu and X. C. Zeng, *J. Chem. Phys.*, 2006, **125**, 154303; S. Bulusu, X. Li, L.-S. Wang and X. C. Zeng, *Proc. Natl. Acad. Sci. U. S. A.*, 2006, **103**, 8326.
2 J. Jellinek and P. H. Acioli, *J. Phys. Chem. A*, 2002, **106**, 10919.
3 A. Lyalin, I. A. Solovyov, A. V. Solovyov and W. Greiner, *Phys. Rev. A*, 2003, **67**, 063203.
4 M. C. Daniel and D. Astruct, *Chem. Rev.*, 2004, **104**, 293.
5 L. Schlapbach and A. Züttel, *Nature*, 2001, **414**, 353.
6 R. W. P. Wagemans, J. H. van Lenthe, P. E. de Jongh, A. J. van Dillen and K. P. de Jong, *J. Am. Chem. Soc.*, 2005, **125**, 16675.
7 P. Larsson, C. M. Araujo, J. A. Larsson, P. Jena and R. Ahuja, *Proc. Natl. Acad. Sci. U. S. A.*, 2008, **105**, 8227.
8 T. H. Dunning, Jr, *J. Chem. Phys.*, 1989, **90**, 1007; D. E. Woon and T. H. Dunning, Jr, *J. Chem. Phys.*, 1993, **98**, 1358.
9 E. J. Bylaska, W. A. de Jong, K. Kowalski, T. P. Straatsma, M. Valiev, D. Wang, E. Aprà, T. L. Windus, S. Hirata, M. T. Hackler, Y. Zhao, P.-D. Fan, R. J. Harrison, M. Dupuis, D. M. A. Smith, J. Nieplocha, V. Tipparaju, M. Krishnan, A. A. Auer, M. Nooijen, E. Brown, G. Cisneros, G. I. Fann, H. Fruchtl, J. Garza, K. Hirao, R. Kendall, J. A. Nichols, K. Tsemekhman, K. Wolinski, J. Anchell, D. Bernholdt, P. Borowski, T. Clark, D. Clerc, H. Dachsel, M. Deegan, K. Dyall, D. Elwood, E. Glendening, M. Gutowski, A. Hess, J. Jaffe, B. Johnson, J. Ju, R. Kobayashi, R. Kutteh, Z. Lin, R. Littlefield, X. Long, B. Meng, T. Nakajima, S. Niu, L. Pollack, M. Rosing, G. Sandrone, M. Stave, H. Taylor, G. Thomas, J. van Lenthe, A. Wong and Z. Zhang, *NWChem, A Computational Chemistry Package for Parallel Computers, v. 5.0*, Pacific Northwest National Laboratory, Richland, Washington 99352-0999, USA, 2006.
10 NIST Chemistry WebBook (NIST Standard Reference Database Number 69, June 2005 Release). http://webbook.nist.gov/chemistry/.
11 T. J. Lee, A. P. Rendell and P. R. Taylor, *J. Chem. Phys.*, 1990, **93**, 6636; C. W. Bauschlicher, Jr and H. Partridge, *Chem. Phys. Lett.*, 1999, **300**, 364.
12 A. Ryzhkov and A. Antipin, ViewMol3D 4.34, a 3D OpenGL Viewer for Molecular Structures, http://redandr.tripod.com/vm3/.